September 1, 2008 / Vol. 33, No. 17 / OPTICS LETTERS 1939

Demonstration of defect modes in coupled microresonator arrays fabricated in silicon-on-insulator technology

Candoluasa Y. M. Tobing,[1] Pieter Dumon,[2] Roel Baets,[2] and Mee-Koy Chin[1,*]

[1]Nanyang Technological University, 50 Nanyang Avenue, 639798, Singapore
[2]Ghent University, Sint-Pietersnieuwstraat 41, 9000 Gent, Belgium
[*]Corresponding author: eumkchin@ntu.edu.sg

Received 12 June 2008; revised July 15, 2008; accepted July 21, 2008;
posted July 28, 2008 (Doc. ID 97392); published August 19, 2008

We show experimentally the existence of defect modes in mutually coupled microring resonator arrays fabricated in silicon-on-insulator technology. The movements of donor-like and acceptor-like modes are demonstrated for various defect lengths, in good agreement with earlier theoretical prediction. © 2008 Optical Society of America

OCIS codes: 350.4414, 230.4555.

Microring resonator is an integrated-optic form of Fabry–Perot etalon that is capable of realizing various active and passive functionalities, such as filters, lasers, sensors, and switches. These functionalities can be further extended by integrating these resonators in array geometries for slow-light structure [1,2] and high-order filters [3–5]. In periodic array geometries consisting of identical rings, there exists a frequency band within which the light is not allowed to propagate inside the structure. This is a photonic bandgap (PBG) mechanism that bears a remarkable resemblance to the electronic bandgap in solid-state physics. Similar to its electronic counterpart, introducing irregularities (or defects) inside the structure may excite a defect mode where light is localized near that defect. The concept of a defect mode is not new and has been demonstrated in conventional PBG structures [6], where the defect is usually in the form of a hole of different size or a dislocation [7,8]. However, to our knowledge the concept of defect modes in periodic arrays of microring resonators has not been extensively explored. This structure is somewhat different because of the hybrid properties of PBGs and resonators. Previously we have theoretically demonstrated the existence of defect modes in such hybrid structures [9], and in this paper we present for what we believe to be the first time the experimental realization of the defect modes, verifying the existence of acceptor and donor modes, in microring resonator arrays fabricated in silicon-on-insulator technology.

As shown in Fig. 1(a), our configuration consists of a series of mutually coupled microring resonators with a defect ring at the center of the structure. The defect in our configuration is a ring with different size. The relative size of the defect ring from the regular rings, $dL_D = L_{\text{defect}} - L_{\text{CAV}}$, determines the type of "doping" in the structure. The introduction of a (larger/smaller) defect ring is analogous to doping a donor (acceptor) energy level in electronic band structure.

The detailed model for such an optical structure is as shown presented in [9]. In the absence of the defect ring ($dL_D = 0$), it is shown that such a configuration exhibits a photonic band structure given by the dispersion characteristics $\cos k\Lambda = (1/t)\sin[\omega n_{\text{eff}} L_{\text{CAV}}/(2c)]$, where L_{CAV} is the ring circumference, c is the speed of light in vacuum, n_{eff} is the effective index of the waveguide, k is the Bloch wave vector, t is the amplitude coupling coefficient between adjacent rings, and $\Lambda = L_{\text{CAV}}/2$ is the period of the unit cell. This type of periodic structure is sometimes referred to as a coupled resonator optical waveguide (CROW).

Figure 1(b) shows the dispersion relation of a typical CROW structure of a particular resonance orders ($m = \omega/\Delta\omega_{\text{FSR}}$). When the resonators are on resonance, the cavity modes from individual rings interact and create a continuous band centralized at resonance ($\omega/\Delta\omega_{\text{FSR}} = m$), and the light can propagate in the structure with the group velocity proportional to the coupling factor (t). When the resonators are off resonance, the Bloch wave vector k becomes imagi-

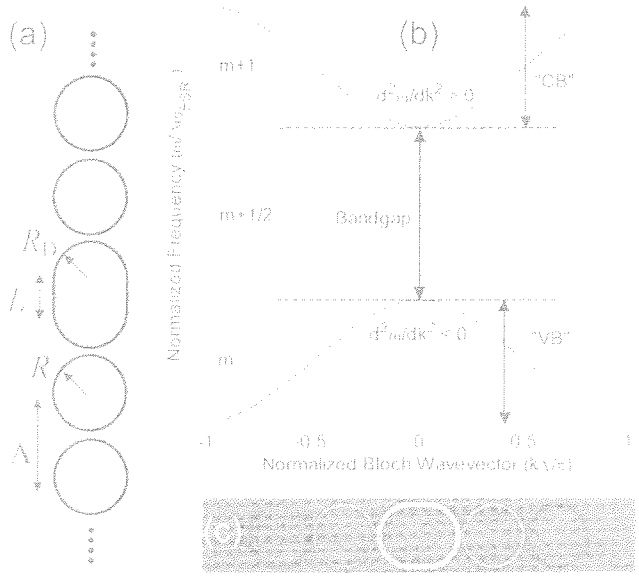

Fig. 1. (Color online) (a) Schematic of a defect mode configuration in a ring-resonator periodic array, (b) band structure of CROW, (c) finite-difference time-domain simulated field distribution in and near the defect ring when a Gaussian pulse is injected from an input waveguide.

0146-9592/08/173939-3$15.00/0

nogy and a PBG is formed, centered at the antiresonance frequency $(\omega/\Delta\omega_{\text{bandgap}}=m+1/2)$. The light then is reflected from the structure in the bandgap region. The difference between this hybrid structure and the conventional PBG is the fact that the bandgap develops faster because the resonator resonantly enhances the reflection in each cell. Thus, fewer cells are required to give the same bandgap properties.

The curvature of the continuous band $(d^2\omega/dk^2)$ determines the type of the mode: positive (negative) curvature is analogous to the conduction (valence) band in electronics. As is apparent in Fig. 1(b), there is always a pair of conduction and valence bands for every resonance order. If one introduces a defect ring inside the structure, then it is possible to have strong light localization in the vicinity of such a defect. As verified by the finite-difference time-domain simulation shown in Fig. 1(c), the light is strongly localized near the defect ring and decays with distance from the defect. The type of defect mode depends on the type of doping introduced. If the defect ring is a smaller ring, then an acceptor-like mode is excited from the valence band (VB). Similarly, if the defect ring is larger, then a donor-like mode is excited from the conduction band (CB). In the finite structure, the Q factor of the defect resonance depends on its relative location from the continuous bands. The Q is higher when the resonance is farther from the continuous bands owing to stronger reflection from the periodic subarrays. The reflection is nearly 100% at the center of the bandgap for *finite* structures, and thus theoretically can give near infinite Q factors. However, in the presence of loss the amplitude of high Q resonance is quickly degraded.

To experimentally demonstrate the existence and dispersion of these defect modes, we designed a set of mutually coupled microring arrays, each with four identical rings and one defect ring at the center (see Fig. 1c). The number of rings is kept low in order to limit the effect of loss in the measurement. The devices were fabricated using a deep-UV complimentary metal-oxide semiconductor process in silicon-on-insulator technology [10]. The waveguide width is 450 nm, and the silicon core thickness is 200 nm. The

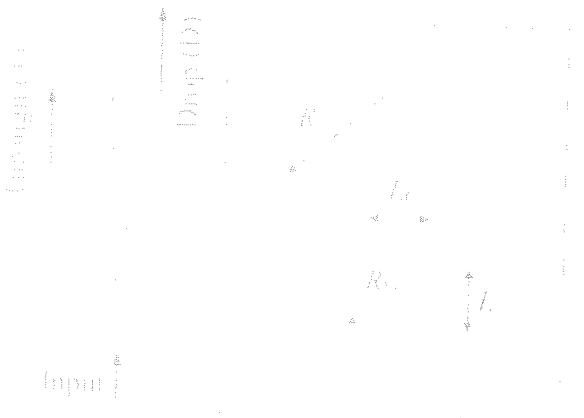

Fig. 2. (Color online) Fabricated devices showing the defect ring in the center of the four-ring array coupled to two waveguides. The defect parameter k_D is controlled by varying L or R_D.

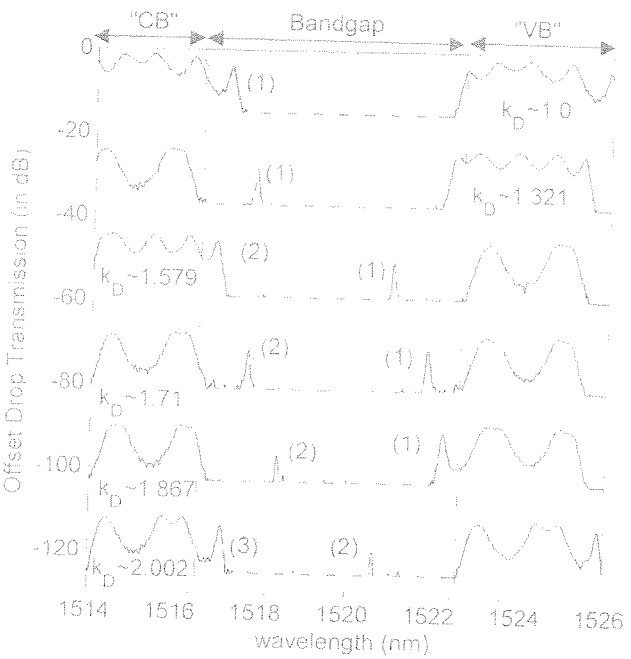

Fig. 3. (Color online) Traces of how donor modes shift in wavelength with increasing defect size. The dashed curves indicate the theoretical fitting of each device.

ring radius is 8 μm. The couplings between the rings and between the input waveguide and the ring are introduced by racetrack coupling of length L_C =6 μm, which is designed to give a fairly large coupling in order to make it easier to excite the defect mode. Finally, to demonstrate the existence of donor and acceptor modes, we varied the defect ring size such that the defect parameter ranges from k_D=0.7 to k_D=2. The defect size is varied by adjusting the extension length (L) and defect radius (R_D) in the defect ring, as shown in Fig. 2.

In the measurements, the device is excited with a broadband source, and coupling into the optical waveguide is facilitated via a second-order grating integrated with the device. The phase-matching condition is achieved when the fiber is butt-coupled to the grating 10° off vertical. The coupling efficiency has a Gaussian spectral profile with a bandwidth of about 30 nm. The output is passed through a 90:10 splitter, where 10% of the power goes to a fiber powermeter for alignment and the rest goes to an optical spectrum analyzer for normalization of the spectrum.

First, we show the traces of donor-like modes in Fig. 3, which plots the measured drop transmissions for increasing defect size. The defect modes are the resonances located within the bandgap region. For clarity the transmissions for different defect modes are offset by −22 dB. As the insertion loss is still high, to make the results clearer, we filtered out the underlying noises by setting a lower transmission threshold of −15 dB. In the theoretical fitting, a vertical offset up to 2 dB is used to compensate the additional insertion loss in each measurement, and a fixed group index of about 4.5 is used to adjust the location of the defect mode resonance.

The theoretical fitting for each device is indicated by the dashed curve. Owing to the dispersive proper-

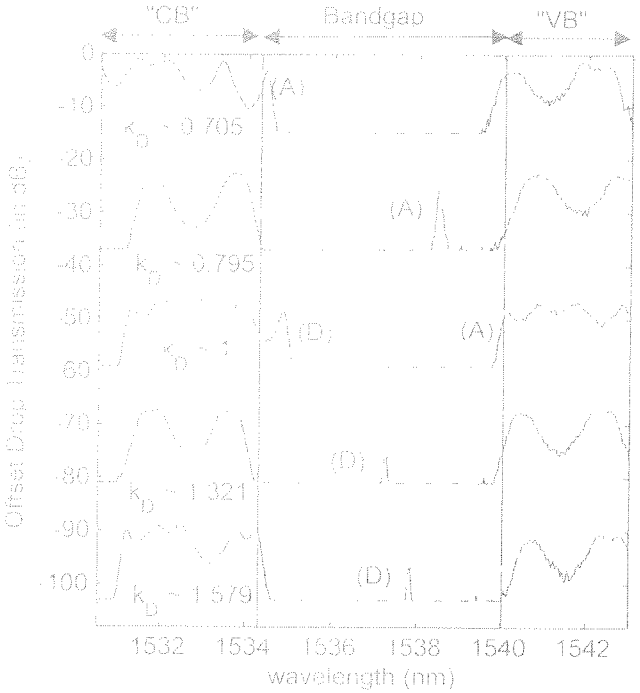

Fig. 4. (Color online) Traces of acceptor (A) and donor (D) modes with varying k_D. The dashed curves indicate the theoretical fitting of each device.

ties of the devices, i.e., because the group index is fixed only for a narrow range of wavelength, a slight horizontal offset between theory and experiment is to be expected. Nevertheless, there is good agreement between theory and experiment. In the fitting, the power coupling factor is found to be ~43%, and the cavity loss is about ~3 dB/cm. These parameters are confirmed with independent measurements from a one-ring two-bus structure with the same racetrack length fabricated in the same sample. The PBG is identified from the low and flat transmission band as indicated in the shaded gray region. The continuous transmission region with shorter wavelength is the CB and that with the longer wavelength is the VB. When the defect ring is only slightly different from the other rings ($k_D \sim 1$), one can observe a defect mode (labeled 1) very close to the conduction band edge. When k_D is progressively increased, mode 1 begins to move from CB to VB. At $k_D \sim 1.7$, a second donor mode (mode 2) emerges near the CB edge, and it moves in the same direction along with mode 1. Finally, in the last graph, where $k_D \sim 2$, we see yet another mode (mode 3) being excited and emerging near the CB.

Finally, we show the traces of both acceptor-like modes and donor-like modes together in Fig. 4, which plots the drop transmissions from smaller ($k_D < 1$) to larger defect ring size ($k_D > 1$). In solid-state physics, an acceptor mode moves from VB to CB when the acceptor level is increased. By analogy, in our photonic structure, the acceptor mode should move to the shorter wavelength with decreasing defect size ($k_D < 1$). Note that this is to be distinguished from the movement of the two donor modes in Fig. 3 that occurs for $k_D \gg 1$. When $k_D \sim 1$, there exist two modes at the CB and VB edges, and we address them as acceptor mode (A) and donor mode (D), respectively. For $k_D < 1$ (the smaller defect rings), mode A shifts to shorter wavelength while mode D is no longer observed. The opposite occurs for $k_D > 1$ (the larger defect rings).

In conclusion, we have demonstrated experimentally the existence of defect modes in a ring-resonator array hybrid structure. Furthermore, by observing the opposite movement of the defect modes for larger and smaller defect ring sizes, we confirm the existence of donor mode (D) and acceptor mode (A) as we predicted in [9]. In addition, we have verified the unique ability of the hybrid resonator structure in generating the PBG with very few unit cells. We observe that the Q of the defect resonance is highest when it is located near the center of the PBG, but the amplitude is also smallest because of the accentuated effect of loss. In general, the Q can be significantly enhanced by slightly increasing the number of unit cells and reducing all the coupling coefficients.

The authors would like to thank Jean Marc Fedelli for fabricating the devices in Commissariat à l'Energie Atomique — Laboratorie d'Electronique de Technologie de l'Information (CEA-LETI) under the e-PIXnet platform.

References

1. A. Yariv, Y. Xu, R. K. Lee, and A. Scherer, Opt. Lett. **24**, 711 (1999).
2. J. K. S. Poon, J. Scheuer, S. Mookherjea, G. T. Paloczi, Y. Huang, and A. Yariv, Opt. Express **12**, 90 (2004).
3. G. Griffel, IEEE Photon. Technol. Lett. **12**, 810 (2000).
4. J. V. Hryniewicz, P. P. Absil, B. E. Little, R. A. Wilson, and P.-T. Ho, IEEE Photon. Technol. Lett. **12**, 320 (2000).
5. B. E. Little, S. T. Chu, P. P. Absil, J. V. Hryniewicz, F. G. Johnson, F. Seiferth, D. Gill, V. Van, O. King, and M. Trakalo, IEEE Photon. Technol. Lett. **16**, 2263 (2004).
6. E. Yablonovitch, Phys. Rev. Lett. **58**, 2059 (1987).
7. S. Fan, J. N. Winn, A. Devenyi, J. C. Chen, R. D. Meade, and J. D. Joannopoulos, J. Opt. Soc. Am. B **12**, 1267 (1995).
8. K. Sakoda and H. Shiroma, Phys. Rev. B **56**, 4830 (1997).
9. Y. Landobasa and M. K. Chin, Opt. Express **13**, 7800 (2005).
10. W. Bogaerts, R. Baets, P. Dumon, V. Wiaux, S. Beckx, D. Taillaert, B. Luyssaert, J. Van Campenhout, P. Bienstman, and D. Van Thourhout, J. Lightwave Technol. **23**, 401 (2005).